Bulletin of the Seismological Society of America, 90, 2, pp. 468–482, April 2000

Source Time Function and Duration of Mexican Earthquakes

by S. K. Singh, J. Pacheco, M. Ordaz, and V. Kostoglodov

Abstract We have compiled source-time functions (STFs) of 54 Mexican earthquakes ($3.0 \leq M \leq 8$). The depth, H, of 48 of these earthquakes lies between 10 and 50 km. The STFs of 43 earthquakes were determined from local and regional strong-motion and/or broadband recordings. For the rest of the events, the STFs were taken from published analysis of teleseismic body waves, or from the University of Michigan Source-Time Function catalog. If available, the seismic moments were taken from the analysis of teleseismic body waves; if not, as was often the case for earthquakes with $M \leq 5.5$, they were estimated from the local recordings themselves. From the STF of each earthquake we have measured pulse duration of each subevent (τ_p), total rupture duration (τ_t), and rise time (τ_r), along with their respective seismic moments. The data fit the relation $M_0/\tau_p^3 \sim 6.7 \times 10^{23}$ dyne cm/s^3. This relation is similar to that reported for deeper earthquakes (mostly in the 50 to 125 km depth range) in the Kanto district of Japan. The pulse duration of Mexican and Kanto earthquakes, scaled to a seismic moment of 10^{26} dyne cm, τ_{ps}, is about 5 s, nearly independent of depth for $10 \leq H \leq 125$ km. We compliment these two data sets with those for California ($H \leq 20$ km) and for deep earthquakes ($H \geq 100$ km). When viewed over the entire depth range, the total rupture duration (τ_t) is related to M_0 by $\log \tau_t = (0.363 \pm 0.008) \log M_0 - 8.58 (\pm 0.190)$, and the duration, within the scatter of the data, appears to be independent of depth. When the data are examined in smaller subsets, as has been done by several authors, certain trends manifest themselves. For example, the pulse and the total duration of deep earthquakes ($H \geq 100$ km) scales as $M_0^{0.16}$ and $M_0^{0.25}$, respectively, and the moment-scaled pulse and total duration decreases by about 20% between 100 and 600 km depth. This decrease is much less than that reported previously. Furthermore, an earlier finding of fast rise times for very deep earthquakes is not substantiated by the recent data. Thus, the anomaly in the duration of the deep earthquakes, as compared to the shallow ones, appears to be smaller than previously suspected.

Introduction

The relationship between seismic moment, M_0, and source duration, τ, provides information regarding the mechanics of faulting in the Earth's interior. For this reason, several researchers have studied the relationship between M_0 and τ. Three measures of source duration of an earthquake have been reported in the literature (Fig. 1): the total rupture duration (τ_t), the pulse duration of each subevent of a complex earthquake (τ_p), and the rise time (τ_r). It is well known that a constant stress drop source model implies that M_0/τ^3 is a constant. For shallow earthquakes the reported values of M_0/τ_t^3 lie between 0.25×10^{23} and 1.0×10^{23} dyne cm/s^3 (e.g., Kanamori and Given, 1981; Furumoto and Nakanishi, 1983; Ekström and Engdahl, 1989; Ekström *et al.*, 1992). These results were obtained from the analysis of teleseismic data. Kikuchi and Ishida (1993) studied source-time function (STF) and subevent pulse duration, τ_p, of earthquakes in the Kanto region of Japan, which were recorded by a broadband seismographic network near the epicentral region. Most Kanto earthquakes had focal depths between 50 and 125 km. Kikuchi and Ishida (1993) reported $M_0/\tau_p^3 \sim 1 \times 10^{24}$ dyne cm/s^3. This value is at least an order of magnitude greater than the values reported for shallow earthquakes in the studies mentioned already.

If τ_{ps} denotes the source duration scaled to a seismic moment of 10^{26} dyne cm, then the relationship between M_0 and τ_p for the Kanto region implies τ_{ps} of about 4.6 sec in the depth range of 50 to 125 km. On the other hand, Vidale and Houston (1993) measured total rupture duration, τ_t, on direct *P*-waves of stacked short-period, vertical-component, teleseismic records of regional networks. They investigated the moment-scaled total rupture duration, τ_{ts}, as function of depth ($H \geq 100$ km) and found that τ_{ts} averaged 11 sec near

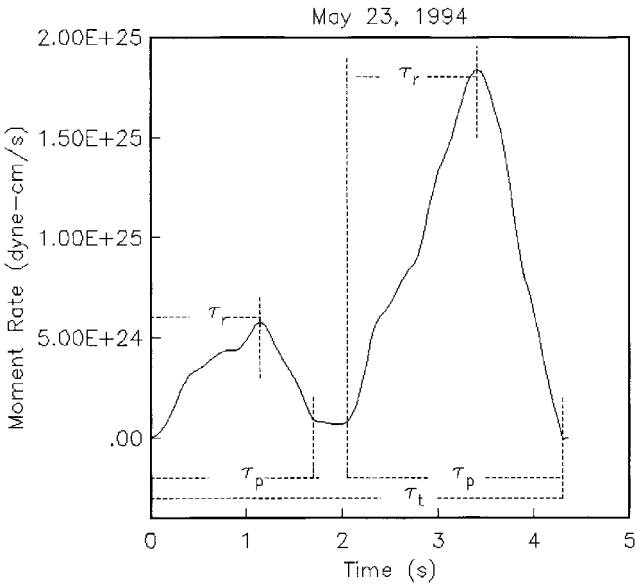

Figure 1. An example of three measures of source duration of an earthquake. The figure shows the STF of 23 May 1994 earthquake (Event 23, Table 1) which consists of two subevents: τ_t, total duration; τ_p, pulse duration of each subevent; τ_r, rise time of the pulse of each subevent.

100 km but decreased to 5.5 sec at ~600 km. Since the moment-scaled duration of shallower Kanto earthquakes (50 ≤ H ≤ 125 km) was about the same as for the deepest earthquakes, it implied that the intermediate-depth earthquakes had anomalously long duration (Singh *et al.*, 1996). Two papers on deep earthquakes report that the decrease in moment-scaled duration with depth is, in fact, small, from 8.5–9.0 s at 100 km to 6.5–7.0 s at 600 km (Bos *et al.*, 1998; Houston *et al.*, 1998). This seems to eliminate the possibility that the intermediate-depth events have abnormally long duration as compared to shallower and deeper earthquakes. However, there still remain several outstanding questions related to the depth-dependence of the duration. In particular, it is important to know whether the reported difference in the M_0 and τ^3 relationship for shallow earthquakes and somewhat deeper Kanto earthquakes is real or is a consequence of the difference in the data set and techniques used in the analysis. Similarly, it is important to know the cause of the discontinuity near 100-km depth in the moment-scaled pulse duration estimated from local and regional data (~4.8 sec) and that obtained from teleseismic data (~8.5 to 9.0 sec). Also, it seems worthwhile reexamining the depth dependence of the duration over the entire depth interval of 10 to 670 km to know if there is a distinct seismic signature of deep earthquakes.

To provide answers to some of the questions raised here, we obtain STFs of Mexican earthquakes. This permits us to establish the relationship between M_0 and τ of relatively shallow Mexican earthquakes. We then compliment the data set from Mexico with those from California and Kanto (Japan), thereby extending the depth range to about 125 km. As the durations in these three data sets have been estimated almost entirely from the analysis of local/regional seismograms using similar techniques, they are directly comparable. We finally analyze the moment-scaled duration (τ_{ps}, τ_{ts}, and τ_{rs}) of earthquakes from Mexico, Japan, and California to investigate how the duration of these shallower earthquakes ($10 \leq H \leq 125$ km) relate to those of the deeper ones ($100 \leq H < 650$ km) reported by Bos *et al.* (1998) and Houston *et al.* (1998).

Data and Analysis

The data on source duration and seismic moment (M_0) of Mexican earthquakes (Table 1) have been compiled from the analysis presented in this article and from other published articles. Table 1 gives the pulse duration, τ_p, and the seismic moment, M_0, of these earthquakes. For complex events the table lists total duration, τ_t, and the total M_0 of the earthquake, as well as pulse duration, τ_p, and M_0 of the individual subevents. The locations of the earthquakes are shown in Figure 2. For large and great earthquakes, the values of τ_t, τ_p, and M_0 have been taken from the analysis of teleseismic body waves. For some moderate earthquakes M_0 is taken from the Harvard CMT catalog, while τ_t and τ_p are estimated from local seismograms.

For a majority of small and moderate earthquakes, we have estimated duration and seismic moment from data recorded at short focal distance. Since its installation in 1985, the Guerrero Accelerograph Array (GAA), located above a segment of the Mexican subduction zone, has produced local recordings of many small, moderate, and large earthquakes (Anderson *et al.*, 1994). Initially the GAA network consisted of 12-bit A/D converters and mostly ± 2 *g* full range accelerometers. It is often difficult to obtain reliable displacement seismograms of small and moderate earthquakes by integrating the accelerograms recorded by these instruments. Beginning in 1996, these accelerographs were gradually replaced by Kinemetrics 19-bit K2 or 18-bit Etna accelerographs. Local accelerograms of small and moderate earthquakes recorded by these instruments can often be directly integrated to obtain displacement seismograms. Presently a network of 18 BB seismographs is also in operation in Mexico. A typical station of BB network consists of a 24-bit Quanterra digitizer connected to Streckeissen STS-2 seismometer and Kinemetrics FBA-23 accelerometer. Local recordings are less frequent by this network because of its sparse nature.

The seismic moments of the earthquakes were estimated either from the low-frequency level of the displacement of *S*-wave spectra or by waveform modeling. In the spectral domain, the inelastic attenuation was corrected by taking $Q_s = 273f^{0.67}$ appropriate for the region (Ordaz and Singh, 1992). The details are given in Ordaz and Singh (1992). Waveform inversion was performed for some events (Table 1). The inversion scheme consisted of a grid search for focal

Table 1
Source Parameters of Mexican Earthquakes Analyzed in This Article

Event No.	Date	Time	Lat (°N)	Long (°W)	Depth (km)	M_0 (dyne cm)	Duration (sec)
1	65/08/23	19:46	16.28	95.80	16	1.90e27‡	16[a]
2	68/08/02	14:06	16.60	97.70	16	8.00e26‡	16[a]
3	73/08/28	09:50	18.30	96.53	80	3.45e26[§,‖]	6[c]
4	78/11/29	19:52	15.80	96.80	18	1.90e27‡	15[a]
5	79/03/14	11:07	17.30	101.40	20	1.00e27‡	17[a]
6	80/10/24	14:53	18.03	96.27	65	6.34e26[‖]	8[‖]
7	81/10/25	03:22	17.75	102.25	27	7.20e26[#]	15[#]
8	82/06/07	06:52	16.35	98.37	20	1.50e26**	10**
9*	85/09/19	13:17	18.14	102.71	17	7.20e27[#]	42[#]
						3.60e27	16
						3.60e27	16
10	85/09/21	05:14	17.62	101.82	22	1.20e27[#]	13[#]
11	86/01/30		18.42	102.99	21	2.00e26[#]	10[#]
12	89/05/02	09:30	16.66	99.49	18	1.90e24††	1.30[#]
13	89/08/12	15:31	18.06	101.13	56	1.31e24††	0.85‡‡
14	90/01/13	02:07	16.82	99.64	16	3.60e23‡‡	1.10‡‡
15	90/05/11	23:43	17.12	100.87	21	2.50e24††	0.65‡‡
16	90/05/31	07:35	17.12	100.87	21	1.10e25†	1.50‡‡
17	90/07/10	06:44	16.83	99.83	23	1.00e23‡‡	0.55‡‡
18	91/05/28	00:56	16.92	99.82	27	7.50e22‡‡	0.38‡‡
19*	92/03/31	19:43	17.22	101.27	11	1.00e24‡‡	1.00‡‡
						0.30e24	0.30
						0.70e24	0.70
20	93/05/15	03:09	16.43	98.74	16	1.00e24‡‡	1.00‡‡
21*	93/05/15	03:11	16.47	98.72	16	2.00e24‡‡	1.80‡‡
						1.00e24	0.80
						1.00e24	1.00
22	93/10/24	07:52	16.67	98.95	34	1.00e25††	3.75‡‡
23*	94/05/23	01:41	18.02	100.57	50	2.77e25††	4.30‡‡
						5.80e24	1.75
						2.20e24	2.30
24*	94/12/10	16:17	17.98	101.52	58	2.80e25[§§]	5.60[§§]
						1.40e25	2.80
						1.40e25	2.80
25	96/02/29	CPDR			S(17.0)	3.70e20‡‡	0.15‡‡
26	95/09/14	14:04	16.31	98.88	16	1.11e27[##]	13.6[‖]
27	95/09/22	08:36	16.37	99.62	S(19.0)	1.00e22‡‡	0.38‡‡
28*	95/10/09	15:35	18.79	104.47	17	4.90e27[##]	60.0[§§]***
						7.00e26	15.0
						4.20e27	45.0
29	95/10/12	16.52	18.69	104.18	S(17.0)	2.00e21‡‡	0.13‡‡
30	95/10/12	23:34	19.65	104.23	S(17.5)	6.00e21‡‡	0.22‡‡
31	95/10/21	02:38	16.92	93.62	160	4.00e26[##]	22.0[##]
32	95/11/12	07:54	15.87	97.39	S(16.5)	7.00e20‡‡	0.06‡‡
33*	95/12/20	21:52	18.53	101.16	55	8.90e23‡‡	1.9‡‡
						6.60e23	0.94
34	96/02/25	03:08	15.83	98.25	S(10.0)	6.10e26[##]	18.0[##]
35	96/03/26	21:54	16.92	100.93	S(13.0)	1.00e21‡‡	0.20‡‡
36	96/03/27	12:34	16.37	98.30	18	1.20e24†††	0.90†††
37	96/03/27	09:40	16.37	98.30	18	1.40e22‡‡	0.18‡‡
38	96/03/31	23:39	17.14	101.13	S(15.5)	4.00e22‡‡	0.50‡‡
39*	96/03/31	23:44	17.20	101.08	S(16.2)	4.00e21‡‡	0.45‡‡
						1.60e21‡‡	0.15‡‡
						2.40e21‡‡	0.15‡‡
40	96/04/01	07:30	17.27	100.89	S(14.0)	2.50e21‡‡	0.18‡‡
41	96/04/08	11:21	16.62	99.70	S(150)	8.00e20‡‡	0.14‡‡
42	96/05/08	01:24	17.05	100.13	24	2.40e22‡‡	0.40‡‡
43	96/05/08	08:27	17.00	100.12	S(16.0)	1.00e22‡‡	0.40‡‡
44	96/05/08	13:32	17.10	100.11	S(16.5)	2.50e22‡‡	0.40‡‡
45	96/06/08	13:06	16.92	100.24	S(17.0)	4.00e22‡‡	0.20‡‡
46	96/06/21	16:12	18.34	100.32	40	1.60e23‡‡	0.67‡‡

(*continued*)

Table 1
Source Parameters of Mexican Earthquakes Analyzed in This Article (*Continued*)

Event No.	Date	Time	Lat (°N)	Long (°W)	Depth (km)	M_0 (dyne cm)	Duration (sec)
47*	96/07/15	21:23	17.41	101.16	25	1.00e26††	7.0‡‡
						3.10e25	2.5
						5.30e25	3.0
48	96/07/18	08:16	17.54	101.20	S(15.5)	4.00e23‡‡	1.00‡‡
49	96/07/19	09:00	17.35	101.29	45	1.00e23‡‡	0.50‡‡
50*	97/01/21	21:19	16.43	98.22	21	1.20e24‡‡	1.20‡‡
						4.80e23	0.70
						7.20e23	0.70
51	97/12/22	05:22	17.22	101.15	20	1.40e24‡‡	1.60‡‡
52	98/02/25	17:09	17.29	101.09	24	1.70e23‡‡	0.80‡‡
53	98/06/01	07:59	16.85	100.09	26	8.30e22‡‡	0.70‡‡
54	98/07/12	08:11	16.87	100.46	18	2.10e23‡‡	0.71‡‡

*Complex event. Seismic moment and duration of the entire earthquake and each subevent is listed separately.
†The depth of the earthquake is shallow but is not well constrained. The depth in the parenthesis is arbitrarily assigned to fall between 10 and 20 km.
‡Chael and Stewart (1982), from teleseismic, long-period body waves.
§Singh and Wyss (1976), from teleseismic body waves.
‖Gonzalez-Ruiz (1986), from teleseismic body waves.
#Astiz *et al.* (1987), from teleseismic, long-period body waves.
**Astiz and Kanamori (1984), from teleseismic, long-period body waves.
††Harvard CMT catalog.
‡‡This study, from local and regional seismograms.
§§Cocco *et al.* (1997), from local seismograms.
‖Courboulex *et al.* (1997a), from local and regional data.
##University of Michigan STF catalog.
***Courboulex *et al.* (1997b), using an empirical Green's function deconvolution technique and teleseismic surface waves.
†††Singh *et al.* (1997), from local seismograms.

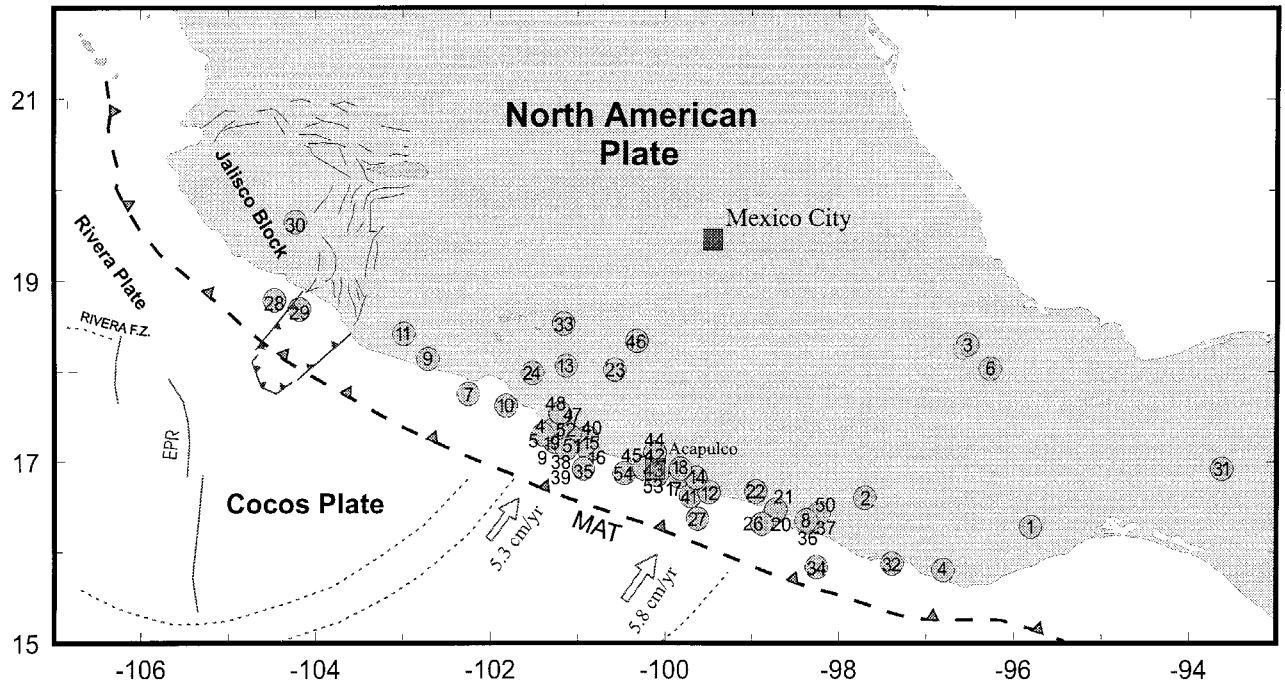

Figure 2. Tectonic map of Mexico showing locations of the earthquakes studied in this article (dark circles). Also shown are Cocos and Rivera plates, Middle America trench (MAT), and East Pacific rise (EPR). Light dashed lines are fracture zones and open arrows indicate relative convergence vector between Cocos and North American plates.

mechanism and M_0 which minimized a misfit function. Theoretical displacement seismograms, needed in the inversion scheme, are for an infinite space and include near-, intermediate-, and far-field terms (Singh *et al.*, 2000). Because the analyzed seismograms were obtained at short epicentral distances, the infinite-space approximation is, generally, valid.

In the far-field, the body-wave displacement pulse is proportional to the STF, provided that the Q effect is negligible. Thus, the STF can directly be obtained from the displacement seismograms. Because P waves are less affected by attenuation than S waves and are less contaminated by the coda, it is preferable to determine the STF from P waves by requiring the area under the P pulse to be equal to M_0. For this reason,whenever possible, we utilized P pulse to obtain the STF. The observed duration is a function of the takeoff angle of the ray and the azimuth of the recording station. When several recordings were available, we took the average value of the source duration. The simplest waveform was taken to represent the shape of the STF. For larger events ($M_w \geq 5$), we estimated the STF using the *SH* pulse.

Figure 3 shows the example of estimation of duration and M_0 of the earthquake of 8 May 1996 (Event 42, Table 1). The P and the *SH* waves at three of the closest stations that recorded the earthquake are illustrated in Figure 3a. The P-pulse shapes and durations are very similar on the three seismograms. The *SH* waves show large variation, mostly because of contamination from P-wave coda. For this event we have chosen the P wave at station CAIG as the STF. Since the STF in this case is simple, τ_t and τ_p are equal (0.4 sec). For an earthquake with a single, near-source recording, the shape and the duration of STF deviate from the true value. This would increase the dispersion in the duration-M_0 plot. However, no consistent bias is expected in the relation. The source displacement spectrum of the earthquake, computed from S-wave, is illustrated in Figure 3. The seismic moment estimated from the low-frequency level of the displacement spectrum is 2.24×10^{22} dyne cm. The waveform inversion (Fig. 3b) gives a seismic moment of 2.40×10^{22} dyne cm, consistent with the spectral estimate.

Two other uncertainties in the estimation of duration arise from the effect of attenuation which (1) increases the pulse duration of the subevents, and (2) makes the visual estimation of the duration subjective. These effects are illustrated in Figure 4 on the simple, theoretical far-field P pulse, computed using Sato and Hirasawa's (1973) circular source model located in an infinite space. In the calculations the observer is located at 25 km from the center of the rupture area, with $\theta = 30°$, $\phi = 0°$, $\alpha = 6.5$ km/sec, $\beta = \alpha/\sqrt{3}$, rupture velocity $V_T = 0.9\,\beta$ and $\rho = 2.8$ gr/cm^3. The calculation of the synthetic P wave requires specification of stress drop. In Figure 4, the τ_p versus M_0 plot, neglecting attenuation, is shown for three values of stress drop, $\Delta\sigma$: 50 bar, 100 bar, and 200 bar. This range of $\Delta\sigma$ covers the average values reported for the region (e.g., Singh *et al.*, 1989, 1990; Castro *et al.*, 1990; Singh and Ordaz, 1994; Humphrey and Anderson, 1994). As expected, τ_p scales with M_0 as $\tau_p \propto M_0^{1/3}$. We include the effect of attenuation by convolving the synthetic P waves with the Futterman's (1962) attenuation operator and an appropriate choice of $t^*(P)$. Although no estimation of $t^*(P)$ is available for the region, it can be roughly estimated from the reported value of $t^*(S)$, which lies between 0.03 sec and 0.034 sec at close epicentral distances (Singh *et al.*, 1989; Humphrey and Anderson, 1992). We note that $t^*(P)/t^*(S) = \beta Q_S/\alpha Q_P$, where Q_S and Q_P are S- and P-wave quality factors. Although Q_S is known for the region (Castro *et al.*, 1990; Ordaz and Singh, 1992), Q_P has not been estimated. We consider two values of Q_P/Q_S: $Q_P/Q_S = 0.83$, reported for hard sites in California (Hough *et al.*, 1988) and $Q_P/Q_S = 9/4$ (Knopoff, 1964). Thus, for a Poisson solid, $t^*(P)/t^*(S)$ may lie between 0.26 to 0.47. Assuming $t^*(S) = 0.034$ sec, the expected value of $t^*(P)$ is between 0.009 sec and 0.016 sec. To evaluate the effect of attenuation on the pulse duration, we take $t^*(P) = 0.016$ sec. We note that $t^* = R/\alpha Q_P$. For $R = 25$ km, and $\alpha = 6.5$ km/sec, the value of $t^* = 0.016$ sec implies $Q_P \sim 240$. The effect of Q gives rise to a seismogram with a long tail, making it difficult to measure τ_p of small earthquakes in an objective manner by visual inspection of theoretical and recorded seismograms. Following Ma and Kanamori (1994), we computed an effective duration, τ_e:

$$\tau_e = [\int f(t)dt]^2 / \int [f(t)]^2 dt \qquad (1)$$

where *f(t)* is the wavelet. In Figure 4, τ_e is shown by solid and open circles corresponding to the effective pulse duration for the unconvolved and convolved synthetic P wave, respectively. We note that, for small earthquakes, τ_e for convolved pulses asymptotically reaches a value of 0.038 sec for $t^* = 0.016$ sec. The figure suggests that for earthquakes with M_0 greater than about 1×10^{22} dyne cm, the effect of attenuation on τ_e may be neglected for $t^* \leq 0.016$ sec and $\Delta\sigma \leq 200$ bars. Since for such earthquakes, the pulse shape and duration are essentially unaffected by attenuation, the measurement of pulse duration, τ_p, directly from the seismogram presents no problem. Thus, as long as we do not consider small earthquakes there is no need to compute τ_e. Although in this article we illustrate the STFs of smaller earthquakes also, we will confine ourselves to events with $M_0 \geq 10^{22}$ dyne cm in establishing the relationship between duration and M_0. We shall measure duration directly from the seismograms. This measure also permits us to compare our results with those reported by most other authors. Figure 5 shows plots of STFs of all earthquakes given in Table 1.

Results

Duration versus Seismic Moment

The plot of τ_p as a function of M_0 is shown in Figure 6a. Assuming M_0 to be proportional to τ_p^3 (a constant stress

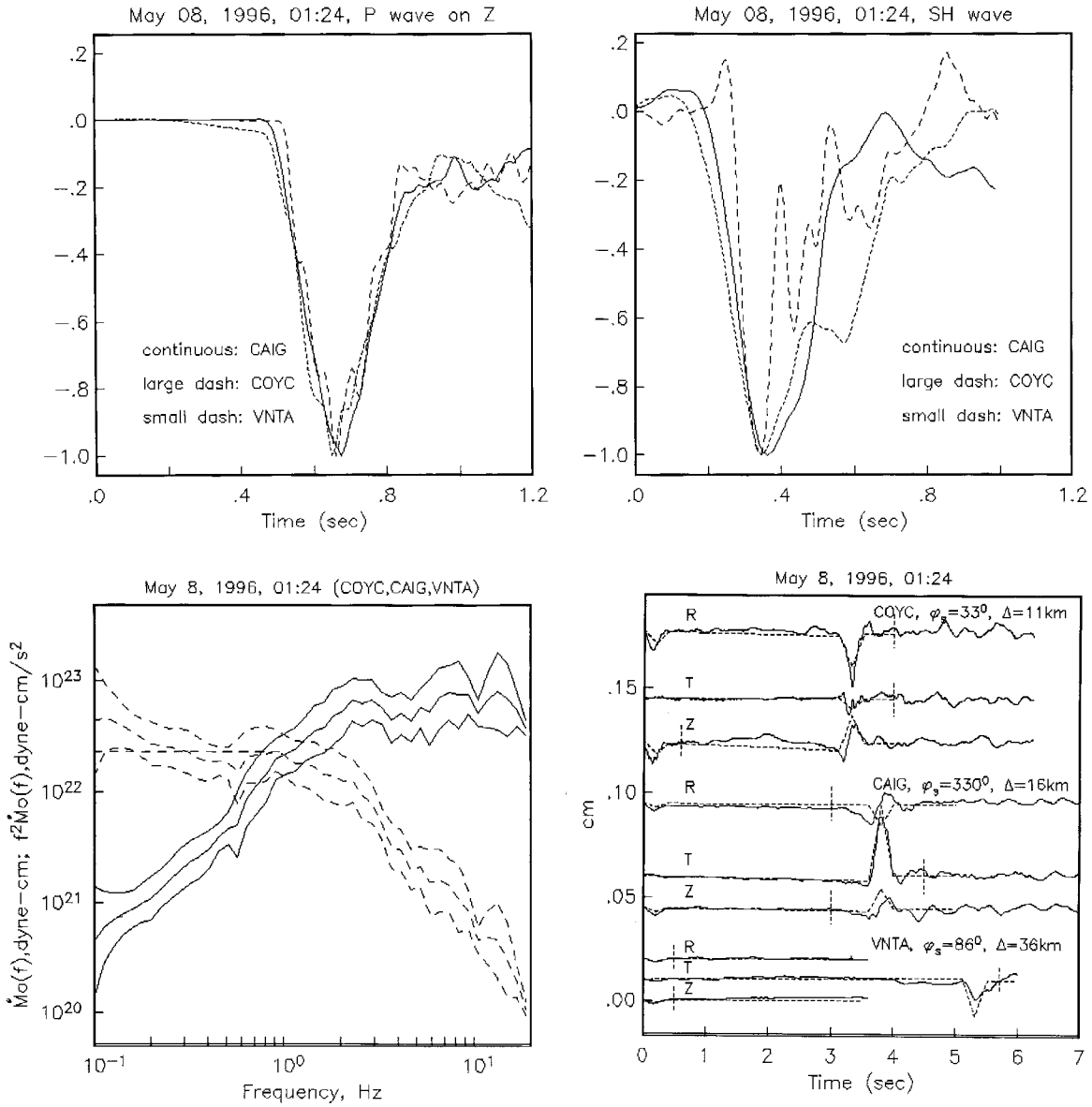

Figure 3. An illustration of estimation of M_0 and source duration of the earthquake of 8 May, 1996 (Event 42, Table 1) Top: Normalized displacement waveforms at stations COYC ($\varphi_s = 33^0$, $\Delta = 11$ km), CAIG ($\varphi_s = 330^0$, $\Delta = 16$ km), and VNTA ($\varphi_s = 86^0$, $\Delta = 36$ km). *P* wave on vertical component (left). *SH* wave (right). The *P* wave on CAIG has been taken as the shape of STF. The source duration is 0.40 s. Bottom: Source displacement (dashed) and acceleration (continuous) spectra (left) estimated from the low-frequency part of the displacement spectra is 2.24×10^{22} dyne cm. Inversion of the waveforms (right). Continuous line: observed seismogram, dashed line: synthetic seismogram. Vertical dashed line shows the duration of the record used in the inversion. The inversion yield $M_0 = 2.4 \times 10^{22}$ dyne cm and a focal mechanism given by $\varphi = 292^0$, $\delta = 13^0$, $\lambda = 85^0$.

drop earthquake source model) and ignoring earthquakes with $M_0 < 10^{22}$ dyne cm, the data are fit by

$$\log \tau_p = (1/3) \log M_0 - (7.94 \pm 0.167). \quad (2a)$$

This relation is shown by straight lines in Figure 6a. We note that this relation also fits data of earthquakes with $M_0 < 10^{22}$ dyne cm. Equation (2a) can be written as:

$$M_0/\tau_p^3 = 6.65 \times 10^{23} \text{ (dyne cm/sec}^3\text{)}. \quad (2b)$$

Equation (2b) is very similar to the relation:

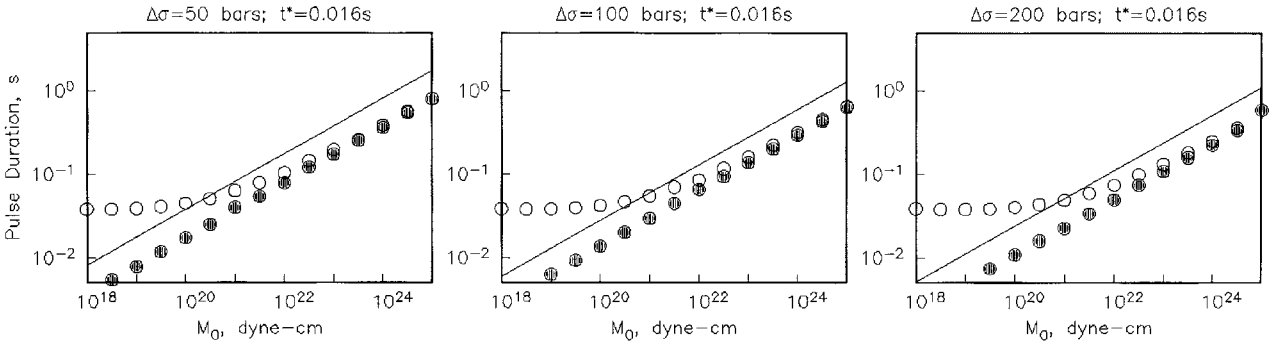

Figure 4. The effect of attenuation on the pulse width of *P* wave. The figure shows pulse duration as a function of M_0. Synthetic *P* waves were computed using Sato's and Hirasawa's (1973) model. Straight line: Pulse width in the absence of attenuation. Solid dots: the "effective" pulse width (see text) in the absence of attenuation. Circles: the "effective" pulse width measured on seismograms convolved with an attenuation operator with t* = 0.016 s. Left, Δσ = 50 bars; middle, Δσ = 100 bars; right, Δσ = 200 bars.

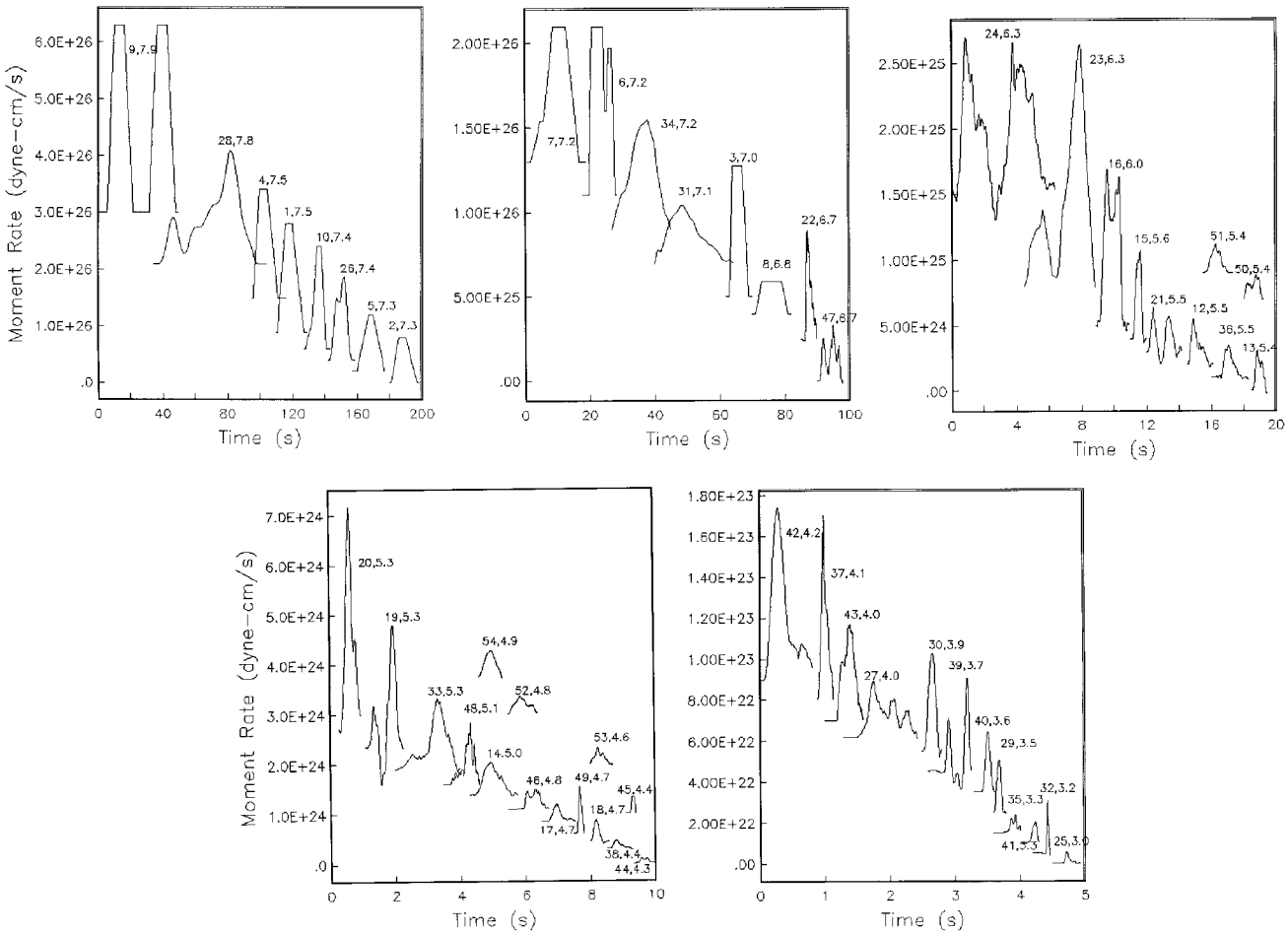

Figure 5. Moment-rate function of Mexican earthquakes listed in Table 1. The pair of numbers associated with each pulse refers to the event number in Table 1 and the moment magnitude, M_w.

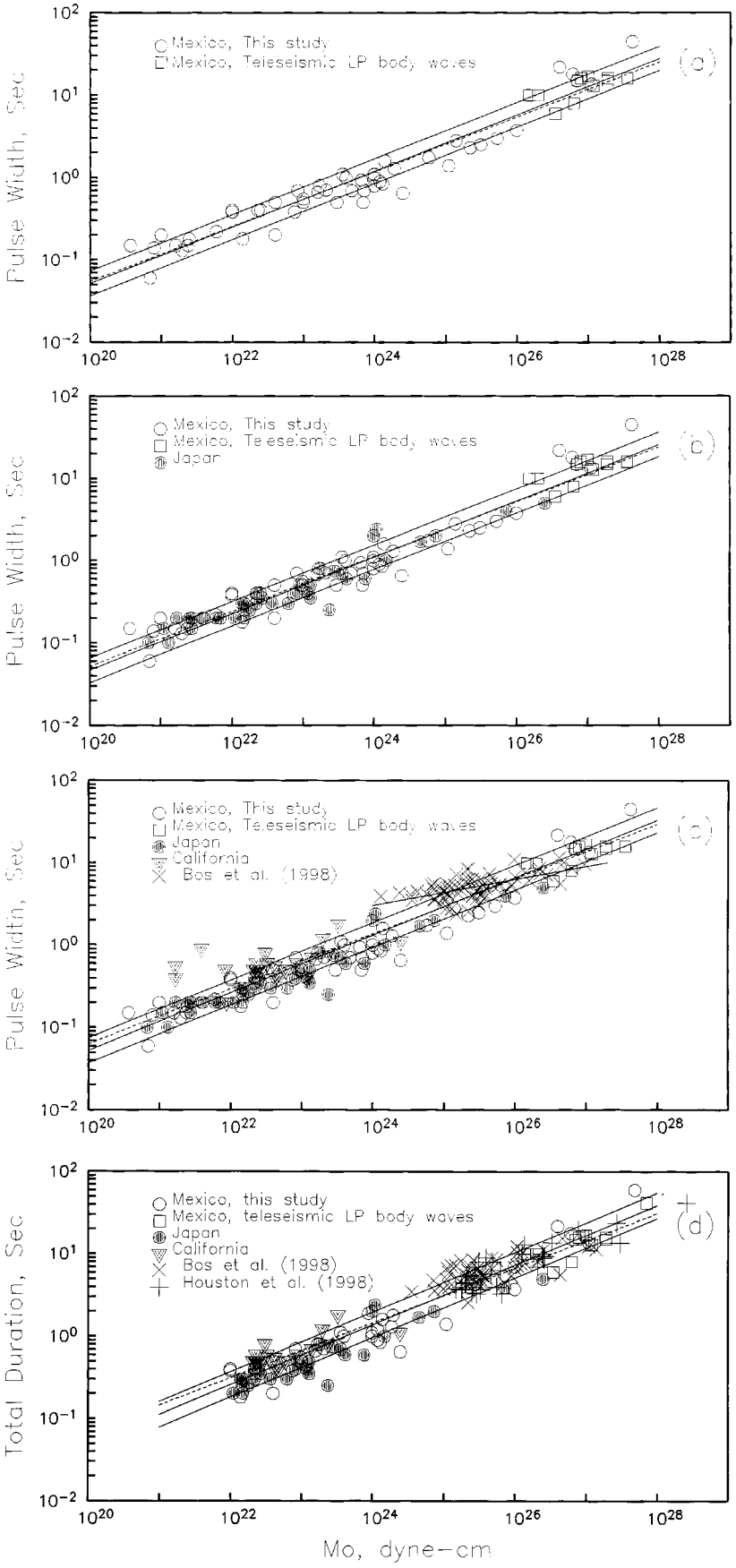

Figure 6. (a) Pulse width (τ_p) versus seismic moment (M_0). Data from Mexico. The best fit and $\pm$ one s.d. are shown by continuous lines. The dashed line shows the fit assuming $M_0 \propto \tau_p^3$ scaling. Only data with $M_0 \geq 10^{22}$ dyne cm are included in obtaining these relations (Table 2). (b) Same as (a) but including data from Kanto, Japan (Kikuchi and Ishida, 1993). (c) Same as (b) but also including data from California (Kanamori *et al.*, 1993; Song and Helmberger, 1997), and from world-wide deep earthquakes (Bos *et al.*, 1998). The regression reported by Bos *et al.* (1998) for deep earthquakes is also shown. (d) Same as (c) but for total rupture duration (τ_t) versus seismic moment (M_0).

$$M_0/\tau_p^3 = 1 \times 10^{24} \text{ (dyne cm/sec}^3\text{)}, \quad (2c)$$

reported by Kikuchi and Ishida (1993) for the Kanto region of Japan. In Figure 6b, Mexican and Kanto data are shown together. The two data sets are indistinguishable from each other. For a circular fault, M_0 and static stress drop, $\Delta\sigma$, are related by $\Delta\sigma = (7M_0/16R^3)$, where R is radius of the fault. Let us assume the rupture velocity to be 0.8 β. Since the duration τ_p roughly equals $2R/0.8\,\beta$ (Cohn *et al.*, 1982) , we can write $M_0/\tau_p^3 = 0.146\beta^3\Delta\sigma$. Taking $\beta = 3.75$ km/sec and 4.46 km/sec, we obtain $\Delta\sigma = 86$ and 77 bars for Mexican and Kanto earthquakes, respectively. We note that most Mexican earthquakes analyzed in this study are shallow ($H < 50$ km) whereas the focal depth of most Kanto earthquakes was between 50 and 125 km. Thus we conclude that there is no significant depth dependence of the pulse duration between 15 to 125 km and the stress drop is roughly the same.

Kikuchi and Ishida (1993) noted that the constant of proportionality between M_0 and τ_p^3, 1×10^{24} dyne cm/sec^3, for the Kanto region is at least one order of magnitude greater than the values reported for shallow earthquakes that lie between 0.25×10^{23} and 1.0×10^{23} dyne cm/sec^3 (e.g., Kanamori and Given 1981, Furumoto and Nakanishi, 1983; Ekström and Engdahl, 1989; Ekström *et al.*, 1992). Kikuchi and Ishida (1993) attributed the difference to (1) higher stress drop of deeper Kanto events, and/or to (2) the relative complexity of shallow earthquakes (so that the estimated values of τ are greater than their expected values corresponding to their seismic moments). As seen from the Mexican data, possibility (1) may be discarded.

In Figure 6c we have added data from California (Song and Helmberger, 1997; Kanamori *et al.*, 1993), and pulse durations of deep earthquakes (H $\geq$ 100 km) listed by Bos *et al.* (1998). California data span a depth range of 1 to 20 km. A somewhat larger scatter in the California data may reflect greater heterogeneity of the shallow crust where these earthquakes originate. The pulse duration of events from Mexico (open circles in Figure 6), Japan, and California have been estimated from local and regional data and, thus, they can be directly compared with each other. Generally, the duration of California events is somewhat larger than for Mexican and Kanto events.

From Figure 6c it can be noted that the pulse durations of the deep earthquakes, which have been estimated by stacking teleseismic broadband seismograms of the global seismograph network, are, on an average, greater than those for Mexican and Kanto earthquakes in the moment range of $10^{24} \leq M_0 \leq 10^{26}$ dyne cm. Bos *et al.* (1998) point out that the pulse duration, τ_p, of the deep earthquakes seems to follow $\tau_p \propto M_0^{0.16}$ scaling, rather than the expected $M_0^{1/3}$ scaling.

Finally in Figure 6d, total rupture duration, τ_t, is plotted as a function of M_0. Only events with $M_0 \geq 10^{22}$ dyne cm are shown. In this figure we have added data from Houston *et al.* (1998), excluding those earthquakes which are included in the data set of Bos *et al.* (1998). While the deep earthquakes alone (shown by crosses and plusses) follow $\tau_t \propto M_0^{1/3}$ scaling (Bos *et al.*, 1998), the entire data set is fit by

$$\log \tau_t = (0.363 \pm 0.008) \log M_0 - 8.580\ (\pm 0.190). \quad (3a)$$

For only the Mexican data the relationship is given:

$$\log \tau_t = (0.363 \pm 0.014) \log M_0 - 8.619\ (\pm 0.337), \quad (3b)$$

which is nearly identical to equation (3a).

A slightly different tendency of deep earthquakes, seen in Figures 6c and 6d, may either be a consequence of the difference in the type of data set (local/regional versus teleseismic) and the methodology used in obtaining the STF, or may reflect a characteristic of such earthquakes.

Depth Dependence of Source Duration

Pulse and Total Rupture Duration. We computed moment-scaled pulse and total rupture durations, τ_{ps} and τ_{ts}, of earthquakes from Mexico, Japan, and California. For Japanese earthquakes, we measured τ_t from the STFs shown in Figure 7 of Kikuchi and Ishida (1993). Assuming $M_0 \propto \tau^3$ (justified by Figure 6), the measured durations were scaled to a seismic moment of 1×10^{26} dyne cm, so that $(\tau_{ps}, \tau_{ts}) = (10^{26}/M_0)^{1/3}(\tau_p, \tau_t)$. The τ_{ps} data from Mexico, Japan, and California is plotted in Figure 7a. The average τ_{ps} for California, Mexico and Japan (shown by horizontal lines in Figure 7a) are 7.3 sec, 5.6 sec, and 4.7 sec, respectively. The data from California and Mexico show larger scatter than the Japan data. Taken together, these data sets suggest a slight decrease in the value τ_{ps} with depth, between 10 and 125 km. In Figure 7b we have included τ_{ts} data for deep earthquakes taken from Vidale and Houston (1993) Based on a preliminary study of STFs of Mexican earthquakes and a plot similar to Figure 7b, Singh *et al.* (1997) suggested that it may be the intermediate-depth earthquakes ($100 \leq H \leq 300$ km), which are the anomalous ones, with relatively large duration, not the deep earthquakes.

Bos *et al.* (1998) (see also Houston *et al.*, 1998) find that most intermediate-depth earthquakes reported in Vidale and Houston (1993) were recorded at large epicentral distances. Bos *et al.* (1998) suggest that the duration of *P* wave at these distances may have been extended due to reflections from D″ layer. Based on $\tau_p \propto M_0^{1/3}$ scaling, these authors report that moment-scaled pulse duration decreases linearly with depth from 9 sec at 100 km to 7 sec at 600 km, a decrease of about 20%, rather than 50% reported by Vidale and Houston (1993). Figure 8a includes the τ_{ps} data from Bos *et al.* (1998), which assumes $\tau_p \propto M_0^{1/3}$. Although the pronounced peak in the τ_{ps} data of Vidale and Houston

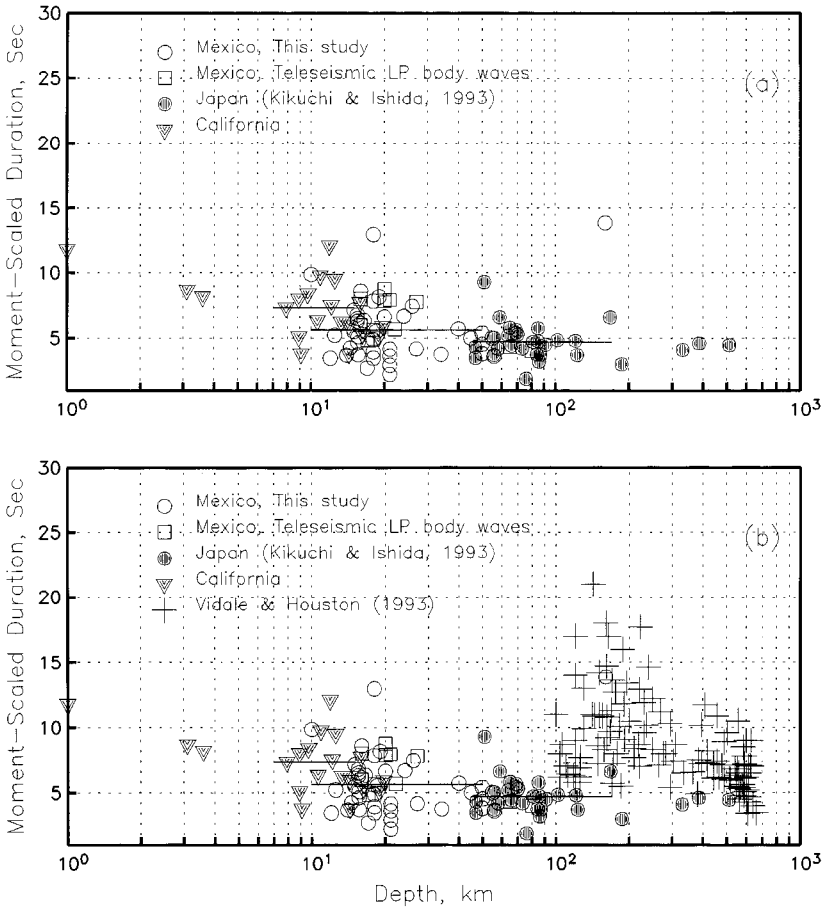

Figure 7. (a) Moment-scaled pulse duration (τ_p), assuming $\tau_p \propto M_0^{1/3}$, normalized to $M_0 = 1 \times 10^{26}$ dyne cm, versus depth. Data from Mexico, Kanto, and California. The horizontal lines show average of Mexican (5.6 s), Japanese (4.7 s), and California data (7.3 s). (b) Same as (a) but including data from deep earthquakes from Vidale and Houston (1993).

(1993) between 100-and 300-km depth is now absent, there is still a discontinuity at 100-km depth between the local/regional and the teleseismic estimates of τ_{ps}; the latter is larger than the former by a factor of about 2. Figure 8b is the corresponding plot for moment-scaled total duration, τ_{ts}.

Why is there a discontinuity in the moment-scaled pulse duration estimated from local/region data and teleseismic data near 100-km depth when the teleseismic data is reduced assuming $\tau_p \propto M_0^{1/3}$ scaling? Why does τ_p of deep earthquakes scale as $\tau_p \propto M_0^{0.16}$? It is beyond the scope of this article to resolve these issues. The discontinuity at 100-km depth, however, suggests a systematic bias in the teleseismic data. The few data points from Kanto region for deep earthquakes, $150 \leq H \leq 500$ km (see Figure 7), are also in accordance with the duration being nearly constant over the entire depth range. Below we consider implications of this possibility on stress drop and apparent stress.

Depth Dependence of Stress Drop/Apparent Stress

For an earthquake of seismic moment M_0 and static stress drop, $\Delta\sigma$, which ruptures a circular area of radius R, $M_0 \propto \Delta\sigma(z)R^3 \propto \Delta\sigma(z)[V_r(z)\tau]^3 \propto \Delta\sigma(z)[C(z)\beta(z)\tau]^3$, where V_r is the rupture velocity, β is the shear-wave speed, and C is a constant that relates rupture velocity to β. Hence,

$$\Delta\sigma(z) \propto M_0/[C(z)\beta(z)\tau]^3, \tag{4a}$$

or,

$$\tau/M_0^{1/3} \propto [1/C(z)\beta(z)\Delta\sigma(z)^{1/3}]. \tag{4b}$$

Let us consider the implications of a constant τ_{ps} over the entire depth range. In this case

$$C_s\beta_s\Delta\sigma_s^{1/3}/C_d\beta_d\Delta\sigma_d^{1/3} \sim 1 \tag{4c}$$

where subscripts s and d refer to average values for shallow ($H < 100$ km) and deep ($H \geq 100$ km) earthquakes, respectively. Let us consider two cases: (1) $C_s \sim C_d$ so that $\Delta\sigma_d/\Delta\sigma_s \sim (\beta_s/\beta_d)^3 \sim (4.45/5.0)^3 = 0.7$ and (2) $\Delta\sigma_s \leq \Delta\sigma_d$, so that $C_d \leq 0.71C_s$. Assuming $C_s = 0.8$, we get $C_d \leq 0.57$. [If we consider that τ_p is constant for $H \geq 100$ km, its value being roughly twice that for $H < 100$ km, then case (1) $C_s \sim C_d$ results in $\Delta\sigma_d/\Delta\sigma_s \sim 0.091$, e.g., the average stress drop of shallow earthquakes is approximately 11 times greater than the deep ones, and case (2) $\Delta\sigma_s \leq \Delta\sigma_d$ yields $C_d \leq 0.45C_s \sim 0.36$.].

Observations on stress drop are subject to large uncer-

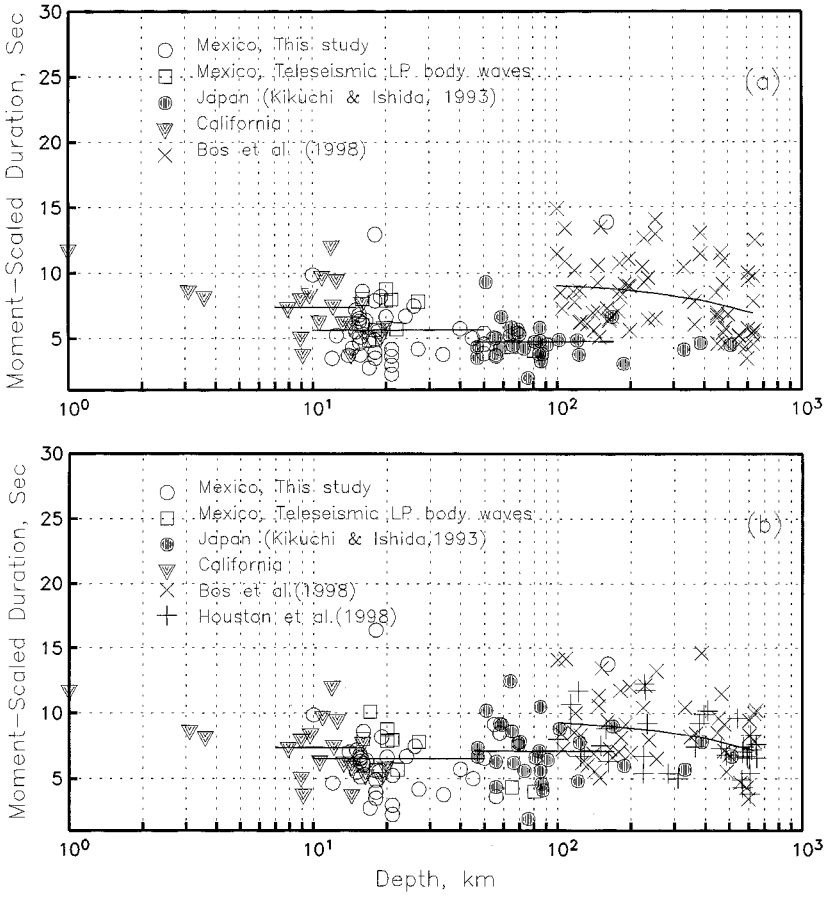

Figure 8. (a) Moment-scaled pulse duration (τ_{ps}), assuming $\tau_p \propto M_0^{1/3}$, normalized to $M_0 = 1 \times 10^{26}$ dyne cm, versus depth. Data for deep earthquakes is from Bos *et al.* (1988). (b) Moment-scaled total duration (τ_{ts}), versus seismic depth, assuming $\tau_t \propto M_0^{1/3}$ scaling. Straight lines show average τ_{ps} for different data sets.

tainty. Indeed, there is no agreement on the depth dependence of the stress drop for intermediate-depth and deep earthquakes (see Frohlich, 1989 for a review). For example, Mikumo (1971) and Sasatani (1980) found an increase of stress drop with depth but Wyss and Molnar (1972) report no change with depth. The stress drop was found to be highly variable at intermediate depth but nearly constant for deeper events by Fukao and Kikuchi (1987). Chung and Kanamori (1980) found that the stress drop was highest near 400-km and 650-km boundaries. Nevertheless, several studies report greater stress drop for deep earthquakes as compared to shallow ones (Molnar and Wyss, 1972, Wyss and Molnar, 1972, Fukao and Kikuchi, 1987; Kikuchi and Fukao, 1987). This observation supports case 2 above, implying that C, the ratio of rupture-to-shear-wave velocity, is smaller for deep earthquakes as compared to the shallow ones. Smaller C values for deep earthquakes has also been suggested by Abe (1982). For the 1994 deep, Bolivian earthquake ($M_w = 8.3$, $H = 637$ km), Kanamori *et al.* (1998) estimate $C = 0.2$. Although this supports case 2, it is not known whether C is small for most deep earthquakes.

A more robust measure of stress associated with earthquake source process is the apparent stress, σ_a, which is defined as $\sigma_a = \mu\,(E_s/M_0)$, where E_s is the radiated seismic energy and μ is the rigidity (Wyss and Molnar, 1972). For Mexican earthquakes, Singh and Ordaz (1994) estimated median value of E_s/M_0 as 7×10^{-5}, and $\sigma_a \sim 24$ bars. For California earthquakes, Kanamori *et al.* (1993) find that $E_s/M_0 \sim 5 \times 10^{-5}$ and $\sigma_a \sim 15$ bars. Houston and Williams (1991) estimated the median apparent stress of deep earthquakes ($100 \leq H \leq 660$ km) to be about 10 bars, independent of depth. Kanamori *et al.* (1993) and Houston and Williams (1991) actually plot the Orowan stress drop, which equals $2\sigma_a$. Abe (1982) reported a nearly constant σ_a for intermediate-depth and deep earthquakes. (In Abe's study E_s was not computed directly but was estimated from the magnitude m_B). Because of the difference in the data used (local/regional versus teleseismic) and the technique employed in the estimation of the seismic energy release, the results of these studies may not be directly comparable. For example, Singh and Ordaz (1994) suggest that for shallow, thrust earthquakes along the Mexican subduction zone, the E_s estimated from teleseismic P waves is smaller than the value obtained from local and regional data. If, however, there is no consistent difference between local and teleseismic estimation of E_s, then the apparent stress is nearly constant over the entire depth range of earthquakes. This is in agreement with a constant moment-scaled duration, independent of depth.

We conclude that the assumption of constant duration

does not lead to any contradiction with the available data on stress and apparent stress.

Rise Time. Houston and Williams (1991) reported that the moment-scaled rise time, τ_{rs}, of earthquakes deeper than about 450 km is about half of those with depth between 100 and 450 km. Here we investigate the depth dependence of the rise time over the entire depth range. Figure 9a shows rise time (defined as the time interval between the beginning of the rupture and the maximum of the moment rate function), scaled to $M_0 = 1 \times 10^{26}$ dyne cm, as a function of depth. The data are from Mexico (Table 2, except for earthquakes whose STF were obtained from modeling of long-period, teleseismic body waves), Kanto region of Japan (measured from Figure 7 of Kikuchi and Ishida, 1993), California (Figure 5 of Song and Helmberger, 1997), and for deep earthquakes (Table 1 of Bos *et al.*, 1998). Only earthquakes with $M_0 \geq 10^{22}$ dyne cm are shown in the figure. For a complex event, the rise time and M_0 of each subevent has been considered separately. Figures 9b and 9c present a closer view of the rise time versus depth of shallow ($H <$ 100 km) and deep ($H \geq 100$ km) earthquakes, respectively. It is possible that the rise time of very shallow earthquakes of California is somewhat larger than the earthquakes of Mexico and Kanto. However, there are too few events to ascertain this. In Figure 9c we have included the rise-time

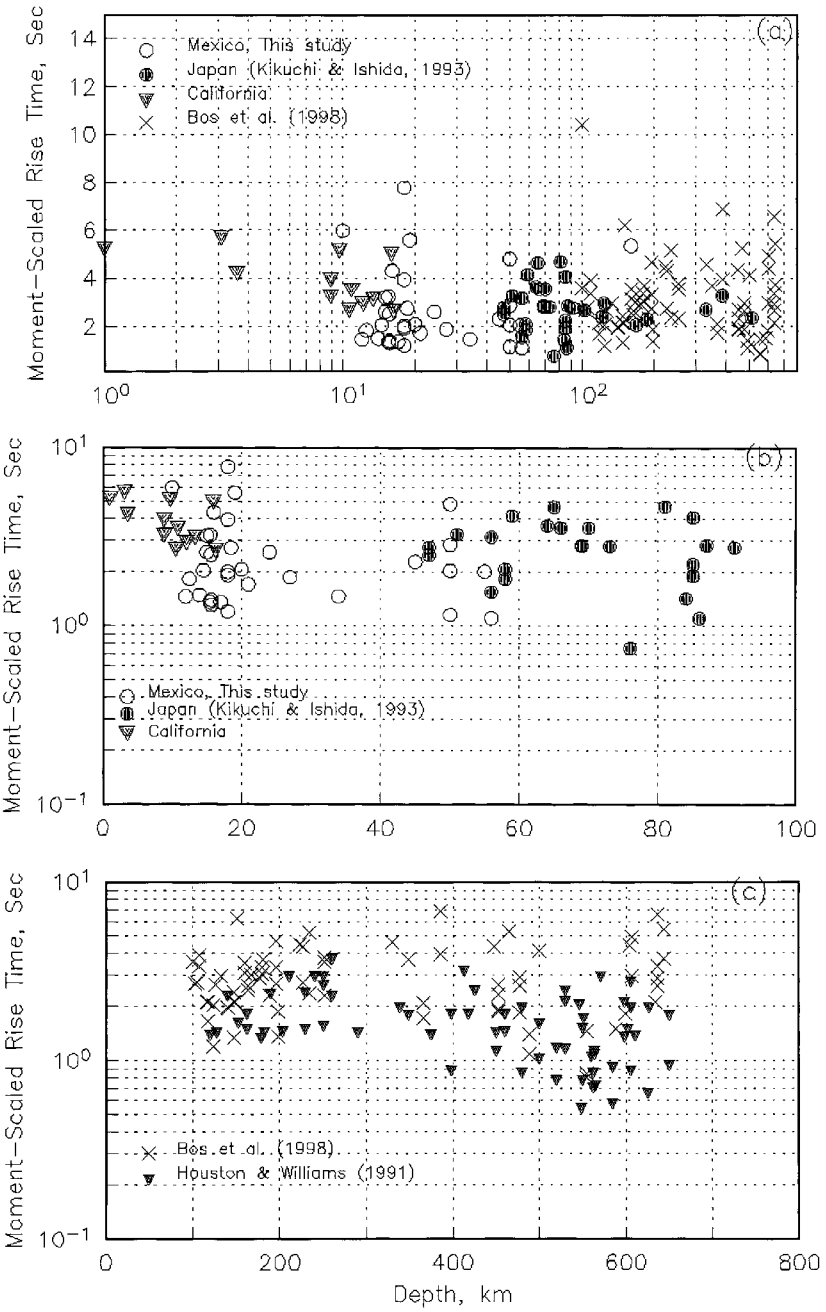

Figure 9. (a) Moment-scaled rise time, normalized to $M_0 = 1 \times 10^{26}$ dyne cm, versus depth, assuming $\tau_r \propto M_0^{1/3}$ scaling. (b) Same as (a) but for shallow events ($H < 100$ km) only. (c) Same as (a) but for deep earthquakes ($H \geq 100$ km) only, including data from Houston and Williams (1991).

Table 2
Results of Regression, $\log \tau = c \log M_0 + d$

Region	Pulse Duration ($\tau = \tau_p$)	Total Duration ($\tau = \tau_t$)
Mexico	$c = 0.342 \pm 0.010$, $d = -8.132 \pm 0.247$	$c = 0.363 \pm 0.014$, $d = -8.619 \pm 0.337$
	$c = 1/3$(fixed), $d = -7.933 \pm 0.164$	$c = 1/3$(fixed), $d = -7.886 \pm 0.172$
Mexico and Kanto	$c = 0.343 \pm 0.009$, $d = -8.196 \pm 0.215$	$c = 0.365 \pm 0.011$, $d = -8.706 \pm 0.262$
	$c = 1/3$(fixed), $d = -7.955 \pm 0.160$	$c = 1/3$(fixed), $d = -7.931 \pm 0.170$
Mexico, Kanto, California, and deep	$c = 0.349 \pm 0.008$, $d = -8.258 \pm 0.194$	$c = 0.363 \pm 0.008$, $d = -8.580 \pm 0.190$
	$c = 1/3$(fixed), $d = -7.866 \pm 0.177$	$c = 1/3$(fixed), $d = -7.843 \pm 0.169$

*M_0, dyne cm, τ sec.

data of Houston and Williams (1991). Curiously, the fast rise time of very deep earthquakes reported by Houston and Williams (1991) and seen in Figure 9c is not supported by the data of Bos *et al.* (1998).

Conclusions

The pulse duration, τ_p, and the seismic moment, M_0, of Mexican earthquakes, in the depth range of ~10 to 50 km, are related by $M_0/\tau_p^3 = 6.65 \times 10^{23}$ (dyne cm/sec^3), so that the median stress drop is about 85 bars. This relation is close to the relationship of $M_0/\tau_p^3 = 1.0 \times 10^{24}$ (dyne cm/sec^3) for earthquakes in the depth range of ~50 to 125 km, reported for the Kanto region of Japan by Kikuchi and Ishida (1993). As these relations are based on data from local and regional seismograms (in 80% of the cases for Mexico and 100% in the case of Kanto), we consider them to be reliable as well as mutually compatible. This suggests that the average value of M_0/τ_p^3 (and hence the stress drop) is nearly constant in the depth range of 10 to 125 km. This value, $\sim 0.7 - 1.0 \times 10^{24}$ (dyne cm/sec^3), is more than an order of magnitude greater than those previously reported for shallow-depth large earthquakes. There are two possible causes for this discrepancy. (1) The modeling of teleseismic body waves of shallow earthquakes may give rise to an overestimation of the duration. (2) For large/great earthquakes, the reported duration refers to the total rupture duration, τ_t, which often includes several subevents so that $\tau_t > \tau_p$. In the case of Mexico and Japan, each subevent and its M_0 has been considered separately.

Shallow earthquakes involve a normal brittle fracture. Since brittle fracture is not a viable mechanism at greater depth due to high temperature and pressure, other mechanisms have been proposed to explain the occurrence of such earthquakes. For example, intermediate-depth ($70 \leq H \leq 300$ km) events are explained by dehydration of water-bearing minerals (e.g., Rayleigh and Paterson, 1965), and transformational faulting has been proposed as a mechanism for deep earthquakes (Green and Burnley, 1989; Kirby *et al.*, 1991). It seems reasonable to expect that these different fracture mechanisms would give rise to distinct seismic signatures. For this reason we investigated the depth dependence of the rupture duration by merging data from shallow and deep earthquakes. Our analysis of various measures of earthquake duration shows no clear pattern of depth dependence. A discontinuity is seen in the data at a depth of 100 km (see e.g., Figures 8a and 8b). On the average, the duration of deeper earthquakes appears to almost twice that for shallower ones. It may be a consequence of some systematic bias in the durations of deep earthquakes which have been estimated by stacking teleseismic seismograms. If we assume that the duration is independent of depth and the stress drop of deep earthquakes is greater or equal to the shallow ones, then we are led to the conclusion that the rupture velocity as a fraction of the shear-wave velocity, and hence the seismic efficiency, is less for deep earthquakes. This has been previously speculated (e.g., Abe, 1982) and is supported by the 1994 Bolivian earthquake (Kanamori *et al.*, 1998).

We conclude that an examination of the data over the entire depth range shows no clear evidence that the duration of deep earthquakes is significantly different from that of shallow ones. When the data are viewed in smaller subsets, certain trends might emerge. However, previous evidence in favor of distinct seismic signature of deep earthquakes now appears to be less overwhelming. For example, recent data show that the moment-scaled pulse and total duration decreases only about 20% between 100- and 600-km depth (Bos *et al.*, 1988; Houston *et al.*, 1998). This decrease is much less than 50% decrease reported earlier (Vidale and Houston, 1993). Additionally, an earlier finding of fast rise time of very deep earthquakes (Houston and Williams, 1991) is not substantiated by the recent data (see Figure 9c).

Acknowledgments

We thank T. Mikumo and Hiroo Kanamori for their comments. M. Kikuchi, T. Mikumo, and D. Doser kindly revised the manuscript. Francoise Courboulex and Miguel Santoyo participated in the initial phase of the research. The records used in this study were obtained by the Guerrero Accelerograph Array (jointly operated by the Instituto de Ingeniería, UNAM, Mexico, and the University of Nevada, Reno, Nevada) and broadband network operated by the National Seismological Service of Instituto de Geofisica, UNAM. This research was partly supported by DGAPA, UNAM project IN109598, CONACyT project 25403-A, and the European Union (Contract CI1*-CT92-0025).

References

Abe, K. (1982). Magnitude, seismic moment and apparent stress for major deep earthquakes, *J. Phys. Earth* **30**, 321–330.

Anderson, J. G., J. Brune, J. Prince, R. Quaas, S. K. Singh, D. Almora, P. Bodin, M. Oñate, R. Vásquez, and J. M. Velasco (1994). The Guerrero accelerograph network, *Geofis. Int.* **33**, 341–371.

Astiz, L., and H. Kanamori (1984). An earthquake doublet in Ometepec, Guerrero, Mexico, *Phys. Earth Planet. Interiors* **34**, 24–45.

Astiz, L., H. Kanamori, and H. Eissler (1987). Source characteristics of the earthquakes in the Michoacan seismic gap in Mexico, *Bull. Seism. Soc. Am.* **77**, 1326–1346.

Bos, A. G., G. Nolet, A. Rubin, H. Houston, and J. E. Vidale (1998). Duration of deep earthquakes determined by stacking global seismograph network seismograms, *J. Geophys. Res.* **103**, 21059–21065.

Castro, R. R., J. G. Anderson, and S. K. Singh (1990). Site response, attenuation, and source spectra of S waves along the Guerrero, Mexico subduction zone, *Bull. Seism. Soc. Am.* **80**, 1481–1503.

Chael, E., and G. S. Stewart (1982). Recent large earthquakes along the middle American trench and their implications for the subduction process, *J. Geophys. Res.* **87**, 329–338.

Cocco, M., J. Pacheco, S. K. Singh, and F. Courboulex (1997). The Zihuatanejo, Mexico, earthquake of 1994 December 10 (M = 6.6): source characteristics and tectonic implications, *Geophys. J. Int.* **131**, 135–145.

Cohn, S. N., T.-L. Hong, and D. V. Helmberger (1982). The Oroville earthquakes: a study of source characteristics and site effects, *J. Geophys. Res.* **87**, 4585–4594.

Courboulex, F., M. A. Santoyo, J. F. Pacheco, and S. K. Singh (1997a). The 14 September 1995 (M = 7.3) Copala, Mexico, earthquake: a source study using teleseismic, regional, and local data, *Bull. Seism. Soc. Am.* **87**, 999–1010.

Courboulex, F., S. K. Singh, and J. F. Pacheco (1997b). The 1995 Colima-Jalisco, Mexico, earthquake (Mw 8): a study of source process, *Geophys. Res. Lett.* **24**, 1019–1022.

Chung, W., and H. Kanamori (1980). Variation of seismic source parameters and stress drops within a descending slab and its implications in plate mechanics, *Phys. Earth Planet. Interiors* **23**, 134–159.

Ekström, G., and E. R. Engdahl (1989). Earthquake source parameters and stress distribution in the Adak Island region of the central Aleutians Islands, *J. Geophys. Res.* **94**, 15499–15519.

Ekström, G., R. S. Stein, J. P. Eaton, and D. Eberhart-Phillps (1992). Seismicity and geometry of a 100-km long blind thrust 1. The 1985 Kettleman Hills, California, earthquake, *J. Geophys. Res.* **97**, 4843–4863.

Frohlich, C. (1989). The nature of deep-focus earthquakes, *Ann. Rev. Earth Planet. Sci.* **17**, 227–254.

Fukao, Y., and M. Kikuchi (1987). Source retrievals for mantle earthquakes by iterative deconvolution of long-period P waves, *Tectonophysics* **144**, 249–269.

Furumoto, M., and I. Nakanishi (1983). Source times and scaling relations of large earthquakes, *J. Geophys. Res.* **88**, 2191–2198.

Futterman, W. I. (1962). Dispersive body waves, *J. Geophys. Res.* **67**, 5279–5291.

Gonzalez-Ruíz, J. (1986). Earthquake source mechanics and tectonophysics of the middle America subduction zone in Mexico, *Ph. D. Thesis*, University of California, Santa Cruz.

Green, H. W., and P. C. Burnley (1989). A new self-organizing mechanism for deep-focus earthquakes, *Nature* **341**, 733–737.

Hough, S., J. G. Anderson, J. N. Brune, F. Vernon III, J. Berger, J. Fletcher, L. Haar, T. Hanks, and L. Baker (1988). Attenuation near Anza, California, *Bull. Seism. Soc. Am.* **78**, 672–691.

Houston, H., and Q. Williams (1991). Fast rise times and the physical mechanism of deep earthquakes, *Nature* **353**, 520–522.

Houston, H., H. M. Benz, and J. E. Vidale (1998). Time functions of deep earthquakes from broadband and short-period stacks, *J. Geophys. Res.* **103**, 29895–29913.

Humphrey, J. R., and J. G. Anderson (1992). Shear wave attenuation and site response in Guerrero, Mexico, *Bull. Seism. Soc. Am.* **82**, 1622–1645.

Humphrey, J. R., and J. G. Anderson (1994). Seismic source parameters from the Guerrero subduction zone, *Bull. Seism. Soc. Am.* **84**, 1754–1769.

Kanamori, H., and J. W. Given (1981). Use of long-period surface waves for rapid estimation of earthquake source parameters, *Phys. Earth Planet. Interiors* **27**, 8–31.

Kanamori, H., J. Mori, E. Hauksson, T. H. Heaton, L. K. Hutton, and L. M. Jones (1993). Determination of earthquake energy and M_L using Terrascope, *Bull. Seism. Soc. Am.* **83**, 330–346.

Kanamori, H., D. L. Anderson, and T. H. Heaton (1998). Frictional melting during the rupture of the 1994 Bolivian earthquake, *Science* **279**, 839–842.

Kikuchi, M., and Y. Fukao (1987). Inversion of long-period P-waves from great earthquakes along subduction zones, *Tectonophysics* **144**, 231–247.

Kikuchi, M., and M. Ishida (1993). Source retrieval for deep local earthquakes with broadband records, *Bull. Seism. Soc. Am.* **83**, 1855–1870.

Kirby, S. H., W. B. Durham, and L. A. Stern (1991). Mantle phase changes and deep-earthquake faulting in subducting lithosphere, *Science* **252**, 216–219.

Knopoff, L. (1964). *Q. Rev. Geophys.* **2**, 625–660.

Ma, K.-F., and H. Kanamori (1994). Broadband waveform observations on the 28 June 1991 Sierra Madre earthquake sequence (ML = 5.8), *Bull. Seism. Soc. Am.* **84**, 1725–1738.

Mikumo, T. (1971). Source process of deep and intermediate earthquakes as inferred from long-period P and S waveforms. 2. Deep-focus and intermediate-depth earthquakes around Japan, *J. Phys. Earth* **19**, 303–320.

Molnar, P., and M. Wyss (1972). Moments, source dimension stress drops of shallow-focus earthquakes in the Tonga-Kermadec arc, *Phys. Earth Planet. Interiors.* **6**, 263–278.

Ordaz, M., and S. K. Singh (1992). Source spectra and spectral attenuation of seismic waves from Mexican earthquakes, and evidence of amplification in the hill zone of Mexico City, *Bull. Seism. Soc. Am.* **82**, 24–43.

Rayleigh, C. B., and M. S. Paterson (1965). Experimental deformations of serpentine and its tectonic implications, *J. Geophys. Res.* **70,** 3965–3985.

Sasatani, T. (1980). Source parameters and rupture mechanism of deep-focus earthquakes, *J. Fac. Sci. Hokkaido Univ. Ser.* **6**, 301–384.

Sato, T., and T. Hirasawa (1973). Body wave spectra from propagating shear cracks, *J. Phys. Earth* **21**, 415–431.

Singh, S. K., and M. Ordaz (1994). Seismic energy release in Mexican subduction zone earthquakes, *Bull. Seism. Soc. Am.* **84**, 1533–1550.

Singh, S. K., and M. Wyss (1976). Source parameters of the Orizaba earthquake of August 28, 1973, *Geofísica Int.* **16**, 165–184.

Singh, S. K., M. Ordaz, J. G. Anderson, M. Rodríguez, R. Quaas, E. Mena, M. Ottaviani, and D. Almora (1989). Analysis of near-source strong-motion recordings along the Mexican subduction zone, *Bull. Seism. Soc. Am.* **79**, 1697–1717.

Singh, S. K., E. Mena, J. G. Anderson, R. Quaas, and J. Lermo (1990). Source spectra and RMS acceleration of Mexican subduction zone earthquakes, *Pure Appl. Geophys.* **133**, 447–474.

Singh, S. K., J. Pacheco, F. Courboulex, V. Kostoglodov, and M. A. Santoyo (1996). Source duration of Mexican earthquakes, *Abs. Suppl. EOS, Trans AGU* **77**, 518.

Singh, S. K., J. Pacheco, F. Courboulex, and D. A. Novelo (1997). Source parameters of the Pinotepa Nacional, Mexico, earthquake of 27 March, 1996 (Mw = 5.4) estimated from near-field recording of a single station, *J. Seism.* **1**, 39–45.

Singh, S. K., M. Ordaz, J. Pacheco, and F. Courboulex (2000). A simple inversion scheme for displacement seismograms recorded at short distances, *J. Seism.* in press.

Song, X. J., and D. V. Helmberger (1997). Northridge aftershocks, a source study with TERRAscope data, *Bull. Seism. Soc. Am.* **87**, 1024–1034.

Vidale, J., and H. Houston (1993). The depth dependence of earthquake duration and implications for rupture mechanisms, *Nature* **365**, 45–47.

Wyss, M., and P. Molnar (1972). Source parameters of intermediate and deep focus earthquakes in Tonga arc, *Phys. Earth Planet. Interiors* **6**, 279–292.

Instituto de Geofiscia
UNAM, C.U.
04510 Mexico, D.F., Mexico
(S. K. S., J. P., and V. K.)

Instituto de Ingeniería
UNAM, C.U.
04510 Mexico, D.F., Mexico
(M. O.)

Manuscript received 15 June 1999.